analytical chemistry

pubs.acs.org/ac Article

Quantitative Measurement of Multiprotein Nanoparticle Interactions Using NMR Spectroscopy

Joanna Xiuzhu Xu,[†] Md. Siddik Alom,[†] and Nicholas C. Fitzkee*

Cite This: *Anal. Chem.* 2021, 93, 11982−11990 Read Online

ACCESS | Metrics & More | Article Recommendations | Supporting Information

ABSTRACT: An effective intensity-based reference is a cornerstone for quantitative nuclear magnetic resonance (NMR) studies, as the molecular concentration is encoded in its signal. In theory, NMR is well suited for the measurement of competitive protein adsorption onto nanoparticle (NP) surfaces, but current referencing systems are not optimized for multidimensional experiments. Presented herein is a simple and novel referencing system using ^{15}N tryptophan (Trp) as an external reference for ^{1}H−^{15}N 2D NMR experiments. The referencing system is validated by the determination of the binding capacity of a single protein onto gold NPs. Then, the Trp reference is applied to protein mixtures, and signals from each protein are accurately quantified. All results are consistent with previous studies, but with substantially higher precision, indicating that the Trp reference can accurately calibrate the residue peak intensities and reduce systematic errors. Finally, the proposed Trp reference is used to kinetically monitor in situ and in real time the competitive adsorption of different proteins. As a challenging test case, we successfully apply our approach to a mixture of protein variants differing by only a single residue. Our results show that the binding of one protein will affect the binding of the other, leading to an altered NP corona composition. This work therefore highlights the importance of studying protein−NP interactions in protein mixtures in situ, and the referencing system developed here enables the quantification of binding kinetics and thermodynamics of multiple proteins using various ^{1}H−^{15}N 2D NMR techniques.

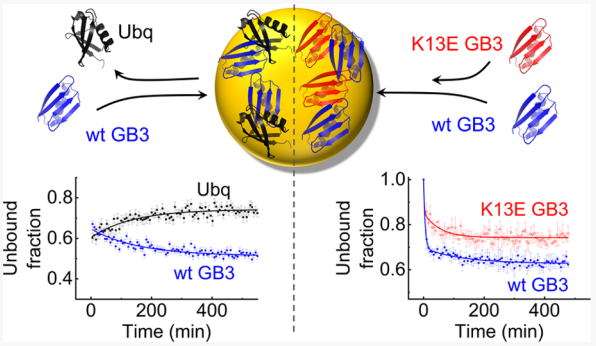

1. INTRODUCTION

The field of nanomedicine has progressed tremendously in recent years, with an increasing number of nanotechnologies being transformed into clinical applications.[1,2] Scientists have functionalized nanoparticles (NPs) with applications in drug delivery, vaccines, biomedical imaging, and sensors.[3−5] However, when NPs are exposed to complex biological fluids such as blood, multiple serum proteins compete and interact with the gold nanoparticle (AuNP) surface immediately, forming a layer of protein on the surface known as the protein corona. Corona formation is recognized as one of the most critical challenges in applied nanotechnologies, and it often leads to the failure of engineered NPs.[6,7] It has been widely accepted in the nanomedicine community that the NP−protein corona, not the functionalized NPs, determines the biological activities and behaviors of NPs.[8] Studies on cell toxicity have shown that the protein corona can promote or inhibit the targeting, circulation time, and cytotoxicity of NPs.[1,9,10] Despite the great amount of effort devoted to understanding protein−NP interactions, quantification of key parameters that govern such interactions has proven to be complex. Effects including charge, hydrophobicity, and binding affinity are known to play a part in protein binding.[11,12] However, currently, it remains impossible to predict the final protein distribution on a NP surface given a mixture of proteins.

As a result, it is highly desirable to monitor the protein behavior in the presence of NPs in situ and in protein mixtures, two necessary components for measuring NP interactions under physiological conditions. Such an investigation would allow monitoring the kinetic and thermodynamic parameters involved in adsorption and how these change over time, for example, during blood circulation.[13] Electrophoretic and mass spectrometric techniques can provide a detailed distribution of numerous proteins on the surface,[14−16] and even information at the level of individual residues,[17] but these destructive approaches require treatments to separate protein−NP complexes and displace the bound proteins, processes that likely alter the observed composition of the protein corona. Multiple non-destructive spectroscopic methods, including fluorescence,[18] circular dichroism,[19,20] cryo-EM,[21] and dynam-

Received: May 5, 2021
Accepted: August 10, 2021
Published: August 25, 2021

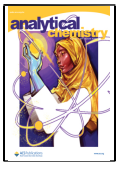

ic light scattering,[22] can be employed in situ, but these methods are normally incapable of disentangling signals from distinct proteins in the corona and therefore not generally suitable for quantifying NP interactions with protein mixtures. Studying protein−NP interactions in mixtures is particularly important, as multiple recent studies show that the binding behavior for a single protein does not necessarily reflect the behavior in the presence of a complex protein mixture. In other words, a reductionist approach will not work for understanding protein−NP interactions. For example, recent research shows that the composition of the protein corona formed in blood serum is not strictly proportional to the individual protein concentrations in serum.[1,16] Moreover, proteins initially adsorbed can be displaced over time by proteins with higher surface affinity but lower concentration.[23,24] Indeed, the kinetic and thermodynamic impacts from other proteins are absent without competition, and studying protein interactions with NPs in mixtures is a key challenge in understanding the NP corona.[12]

In principle, multidimensional nuclear magnetic resonance (NMR) is well suited to the quantitative measurement of protein mixtures in the presence of NPs, as detailed information from each protein residue can be readily quantified. In the study of protein−NP association, the line broadening effect that occurs upon binding is particularly important in studies of protein corona.[25] Multiple outcomes are possible: residues that are weakly coupled to the NP surface can exhibit lifetime line broadening, becoming broader in the presence of NPs.[26,27] In addition, when proteins are intrinsically disordered or contain long, flexible loops, the motions of flexible residues can lead to different broadening behaviors for each residue.[19,28,29] However, for many circumstances, the situation becomes much simpler: when proteins are globular and lack long loops, and when the kinetics of desorption are slow on the NMR time scale,[30] all signals from the adsorbed proteins are uniformly broadened beyond detection. The intensity of the observed NMR signal therefore is proportional to the concentration of free proteins, which can be used to quantify the bound proteins. This situation occurs for proteins in the "hard" corona,[8] and it has been observed for globular proteins binding to the surface of citrate-coated AuNPs.[31,32] In these studies, 1D proton signals were used to quantify the bound proteins, but a suitable and convenient referencing system for multidimensional NMR has not yet been identified. Several properties are needed to fulfill the requirements of such a referencing system, such as a robust, well-resolved signal, and no chemical interactions with the NPs or proteins under investigation. In addition, for absolute quantification of binding, the reference should have a known extinction coefficient to enable facile comparison of concentrations across different samples. Such a reference would allow for the simultaneous monitoring of multiple proteins in the presence of NPs for quantifying binding thermodynamics and kinetics, significantly expanding the ability of NMR spectroscopy to study the multiprotein binding behavior for the hard corona in situ.

In this work, we develop such a standard based on ^{15}N-labeled L-tryptophan, an amino acid with a distinctive indole proton chemical shift and a well-known UV−visible extinction coefficient. The interactions between the reference, proteins, and NPs are eliminated using a commercially available coaxial insert NMR tube. We demonstrate that this system shows similar or better performance to measurements performed using 1D NMR. Then, we explore the advantages offered by this system when measuring complex protein mixtures and binding kinetics, including the challenging case when proteins differing by a single residue compete for the same AuNP surface.

2. EXPERIMENTAL SECTION

2.1. NMR Reagents and Proteins. Tryptophan (^{15}N labeled, NLM-800-PK), deuterated 3-1-propanesulfonic acid-d_6 sodium salt (DSS-d_6, DLM-8206), 99.9% D_2O (DLM-4), and deuterated sodium acetate (NaOAc-d_3, DML-3124) were purchased from Cambridge Isotope Labs (Tewksbury, MA). Wild-type (wt) GB3 and ubiquitin (Ubq) proteins were expressed recombinantly in *Escherichia coli* (BL21) cells and purified as described previously.[32,33] Details for mutagenesis of wt GB3 to obtain K13E GB3 are presented in the Supporting Information.

2.2. Preparation of the Coaxial Standard. The extinction coefficient of the ^{15}N-labeled tryptophan (^{15}N Trp) (MW 206.21 g/mol) is 5500 M^{-1} cm^{-1} at 280 nm. A 2 mM ^{15}N Trp standard solution with 20 mM NaOAc (MW 85.05 g/mol) buffer and 1 mM DSS-d_6 (224.4 g/mol) in 50% D_2O (v/v) is prepared as follows. ^{15}N Trp (4.12 mg), NaOAc (17.00 mg), and DSS-d_6 (2.24 mg) were dissolved in ∼5 mL of 50% D_2O. Then, this ^{15}N Trp standard solution was adjusted to pH 4.0 using a 4 M HCl solution before topping off to 10 mL with 50% D_2O. After preparation, 100 μL of the standard solution was transferred to a coaxial insert tube (WGS-5BL) purchased from Wilmad LabGlass (Vineland, NJ). Before use, the standard was degassed with an aspirator pump by placing the coaxial insert tube in a sidearm flask and applying vacuum for 10−15 min. The coaxial insert tube with the standard solution was stored at 4 °C.

2.3. Synthesis and Characterizations of 15 nm AuNPs. Gold(III) chloride trihydrate (catalog #520918) and sodium citrate dihydrate (#567446) were purchased from Millipore Sigma. The synthesis was performed using the method of Frens and Turkevich.[34,35] Details on AuNP synthesis and characterization are provided in the Supporting Information.

2.4. Determination of Binding Capacity. For binding capacity measurements, 20 μM of ^{15}N-labeled GB3 or ^{15}N-labeled Ubq was mixed with AuNPs with varying concentrations of 0, 20, 40, 60, and 80 nM. The protein peak intensities are measured by 2D TROSY-HSQC experiment[36] on a 600 MHz Bruker AVANCE III NMR system equipped with a CP-QCI cryoprobe. Detailed sample preparation and parameters used for NMR experiments are presented in the Supporting Information.

The fraction (r) of unbound (free) proteins was determined by the ratio of peak intensities of the AuNP-containing samples (I) versus the protein control sample (I_0) for each residue ($r = I/I_0$), after normalization by the ^{15}N-Trp reference peak. The AuNP-bound protein NMR signals will diminish due to its extremely short T_2 relaxation times.[30,31] The concentration of bound proteins ($[\text{protein}]_{\text{bound}}$) was calculated using the total protein concentration ($[\text{protein}]_{\text{total}}$) using the following equation, as described previously[31]

$$[\text{protein}]_{\text{bound}} = (1 - r)[\text{protein}]_{\text{total}} \quad (1)$$

2.5. Competitive Binding between Protein Variants. Competitive binding experiments between 20 μM ^{15}N-labeled wt deuterated GB3 (GB3-D) and 20 μM wt non-deuterated

https://doi.org/10.1021/acs.analchem.1c01911
Anal. Chem. 2021, 93, 11982−11990

GB3 (GB3-H) for 40 nM AuNPs were conducted with a high-resolution TROSY-HSQC experiment to differentiate closely positioned deuterated and protonated peaks.[37] Competitive binding of 20 μM ^{15}N-labeled GB3 and 20 μM ^{15}N-labeled Ubq for 80 nM AuNPs was conducted with the SOFAST-HMQC experiment. The Trp standard was used as the coaxial insert for calibration of peak intensities. Detailed sample preparation and parameters used for NMR experiments are given in the Supporting Information. The ratio of signals from each protein residue with (I) and without (I_0) AuNPs is defined as the normalized intensity (I/I_0), which estimates the fractional unbound protein concentrations (eq 1).

2.6. Kinetics Measurements of Protein Adsorption. The sensitivity-enhanced SOFAST-HMQC experiment[38,39] was selected for monitoring a mixture of two proteins (20 μM GB3/20 μM Ubq and 20 μM wt GB3/20 μM K13E) being adsorbed onto 80 nM AuNPs. Detailed sample preparation, NMR parameters, and an NMR pipe processing script are presented in the Supporting Information.

All residue peak intensities are normalized by the Trp standard prior to further analysis. All kinetic data were fit with a first-order kinetics model with one or two time constants (eq 2) as follows.

$$I/I_0(t) = y_0 + \sum A_i \times e^{-t/\tau_i} \quad (2)$$

where $I/I_0(t)$ is the Trp-normalized relative intensities of the residue peaks at the binding time of t. The intensities at binding time t ($I(t)$) are expressed relative to the residue-specific peak intensities of the protein control sample with no NPs (I_0) for analysis. y_0 is the fitted intercept of the model. The quantitative reference described above allows for the determination of how much signal is lost during the experimental dead time. The time t (in min) is the binding time after adding AuNPs into the protein(s) samples. The time constant τ_i (in min) is the fitted time constant of the ith exponential decay process. All curves were fit using OriginPro (OriginLab).

3. RESULTS AND DISCUSSION

3.1. Quantitative Comparison of Single-Protein Binding. One key requirement of a quantitative NMR study is that the signals of interest must be reliably calibrated by the integral of the reference compound. The reliability of the reference depends mainly on two aspects. First, the reference signal must be robust and strong with a high signal-to-noise ratio (SNR), but not so strong that it overwhelms the signals of interest. Second, the reference signal must be well resolved from other peaks. We first verify the proposed Trp reference by quantification of GB3 binding to AuNPs with a ^{15}N-decoupled proton NMR experiment (Figure 1A). GB3 adsorption to citrate-capped AuNPs has been studied before using trimethylsilylpropanoic acid (TMSP) as an internal reference,[31] and 180 ± 20 GB3 protein molecules were observed to bind to a 15 nm AuNP. Importantly, the line widths do not broaden, and all peaks decrease uniformly, indicating that NMR signals can be used to quantify the binding. We propose to use the Trp indole peak located at 10.5 ppm for a reference signal since it is robust and completely isolated from the protein amide peaks, which appear in the ^{1}H region from 7 to 9.5 ppm. When increasing amounts of citrate-stabilized 15 nm AuNPs were titrated into a constant concentration of GB3 protein, the peak intensities from GB3 linearly decrease due to

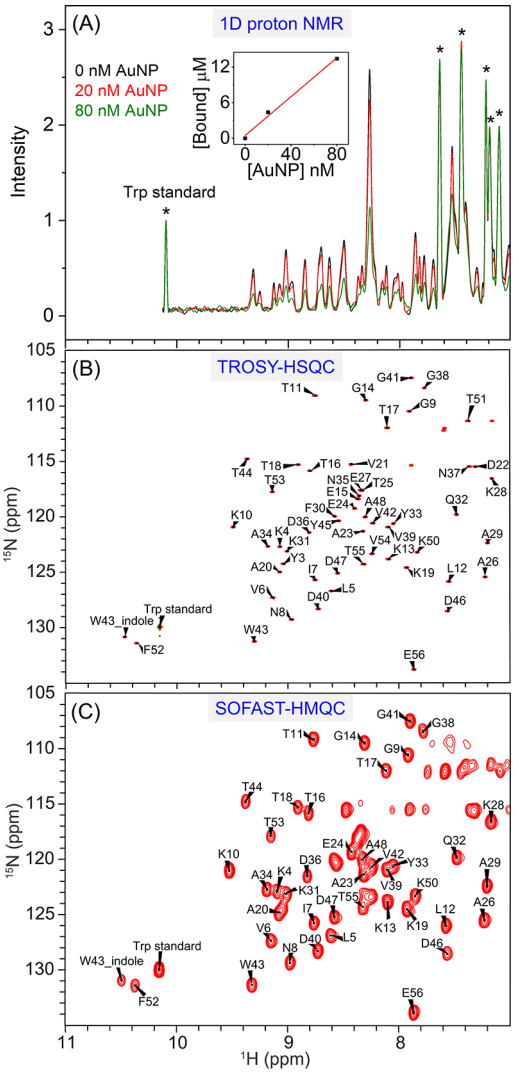

Figure 1. Spectral resolution in 1D and 2D NMR experiments in the presence of the Trp standard. (A) ^{15}N-decoupled 1D proton NMR spectra of 25 μM ^{15}N-GB3 mixing with 0, 20, and 80 nM 15 nm AuNPs. The peaks indicated by asterisks (*) are side-chain proton resonances from the Trp external reference. All spectra are normalized to the intensity of the Trp indole HN proton. The inset shows the calculated bound concentrations of GB3 as a function of AuNP concentration. (B) TROSY-HSQC and (C) SOFAST-HMQC spectra of 20 μM ^{15}N-GB3 with Trp as the external reference compound. The external Trp reference peak is well resolved and labeled "Trp standard". The other GB3 assignments are also labeled.

adsorption onto the AuNP surface (Figure 1A, main spectra). GB3 binding to AuNPs is in the slow exchange regime, and therefore, the amount of bound GB3 should quantitatively correspond to the reduction in the NMR signal intensity.[31] To process the data, all protein signals are normalized by the Trp indole peak to quantify the fraction of unbound proteins and therefore the bound protein concentrations using eq 1. Here, the calculated concentration of bound GB3 increases linearly as a function of added AuNP concentration (Figure 1A, inset), and the binding capacity deduced from the fitted slope is 163 ± 14, which is in good agreement with prior results.[31] It should be noted that there are proton signals in the range of 7−9.5 ppm (highlighted by *) that remain constant regardless of the AuNP concentration. Those peaks belong to the aromatic protons of the Trp reference compound, but they do not

https://doi.org/10.1021/acs.analchem.1c01911
Anal. Chem. 2021, 93, 11982−11990

interfere with measurement of the protein concentration, and they are not visible at all in 2D spectra.

Subsequently, the potential utility of the Trp reference in $^{1}H-^{15}N$ 2D NMR experiments was examined with TROSY-HSQC[40] and SOFAST-HMQC[38,39] NMR techniques (Figure 1B,C). 2D NMR provides residue-specific information that is inaccessible in 1D NMR. In studying protein−NP interactions, the dynamic and conformational perturbations of each residue in the protein backbone upon interactions can be extracted from the ^{1}H or ^{15}N chemical shifts, intensities, and linewidths.[30] The 2D TROSY-HSQC (or standard HSQC) provides high spectral resolution and is ideal for quantitative measurement of complex protein mixtures at equilibrium or steady state. Conversely, the SOFAST-HMQC experiment collects spectra very rapidly (Figure 1C was recorded in 6 min), enabling real-time observation of the dynamic process of protein−NP binding.[38] The spectral resolution of SOFAST-HMQC can be reduced compared to the standard 2D NMR techniques, a result of fewer acquired points in the indirect acquisition dimension.[41] In addition, the SNR of SOFAST-HMQC spectra should be optimized since protein−NP binding experiments often require low concentrations of NPs (<100 nM) and proteins (<100 μM) to reduce aggregation and to maximize the signal change upon binding. The data presented in Figure 1C demonstrate that an appropriate balance of resolution and SNR can be identified, while still achieving fast acquisition times, on the order of minutes. For both spectra in Figure 1B,C, the Trp signal is well resolved. Therefore, this reference should be broadly useful in studying NP binding for a variety of proteins.

In addition to being well resolved, the signal intensity of the Trp reference is also robust in both 2D NMR spectra, making it suitable for peak intensity calibration. For instance, with 20 μM GB3 present, the single indole Trp peak is approximately 5 times more intense than the signals from GB3. While the concentration of ^{15}N-Trp (2 mM) in the reference solution is significantly higher than GB3, its signal is reduced by several factors: first, the coaxial insert reduces the effective concentration of Trp in the sample. Second, the presence of 50% D_2O reduces the Trp indole signal further, as these protons will exchange with the solvent over time. Third, the Trp compound has a longer T_1 relaxation time than the protein signals, resulting in incomplete spin relaxation between scans. This leads to a reduction in the Trp signal that will depend on the recycle delay. However, provided the delay is maintained for both samples with and without NPs, and provided no additional line broadening is observed in the protein, the intensity ratio with/without NPs (I/I_0) used to quantify protein adsorption will be constant (a detailed justification is provided in the Supporting Information). The solubility of the Trp amino acid is 55 mM at 25 °C,[42] so the intensity of this peak can be adjusted by increasing or decreasing the concentration of Trp in the sample solution. Thus, this approach is highly versatile for measuring relative concentrations in a variety of systems and pulse sequences. Additional practical considerations for performing intensity calibration using the Trp standard, including a discussion of zero filling, are outlined in the Supporting Information.

We tested the Trp standard for the quantitative study in 2D NMR by determining the binding capacities for GB3 and Ubq on 15 nm, citrate-capped AuNPs (Figure S5, Supporting Information). As described above, these binding capacities have been quantified previously using 1D NMR and TMSP as an internal referencing standard.[31] In this work, the peak intensities of each residue are measured and calibrated by the external Trp standard prior to data analysis. As observed in 1D NMR, the protein peak intensities of GB3 or Ubq in 2D NMR monotonically decrease as AuNPs are titrated into the protein solution, which corresponds to a linear increase of bound protein (eq 1). This behavior is expected anytime binding is tight (K_d < 1 μM) and slow on the NMR time scale (seconds or longer).[31] These conditions generally apply to globular proteins in the hard corona; if signals do not scale uniformly, or if line broadening is observed, additional analysis must be performed, and simple peak intensities are not sufficient to quantify the adsorbed protein. Here, both GB3 and Ubq signals exhibit a uniform decrease with excellent linearity (R^2 > 0.99). The binding capacities of GB3 (178.1 ± 1.4 proteins per NP) and Ubq (168 ± 4 proteins per NP) were determined as the fitted slope through the origin. Importantly, these values are statistically identical to the previously determined values of 180 ± 20 and 156 ± 12 proteins per NP for GB3 and Ubq, respectively.[31] By comparison, the current approach using 2D NMR with the Trp reference offers better linearity and smaller uncertainties over the previous study using 1D proton NMR with TMSP as the internal reference.

The robustness of the method can be attributed to several factors. First, the 2D NMR approach enabled by the Trp reference provides better resolution than the 1D approaches. Since individual peaks are not resolved in the 1D experiments, an average signal profile is scaled to determine the concentration of bound proteins (Figure 1A), whereas in a 2D spectrum, all signals originating from proteins can be isolated and quantified individually (Figure 1B). This increases the precision in the measured signal. Second, the 2D approach allows for the removal of signals that may originate from buffers or other cosolvents. Not only does this remove confounding signals from non-interacting components and increase accuracy but it also enables the measurement of protein−NP interactions on protonated buffers [e.g., *N*-(2-hydroxyethyl)piperazine-*N*′-ethanesulfonic acid] because proton signals originating from these buffers are not observed in $^{15}N-^{1}H$ 2D correlation spectra. Third, the external referencing system used here is more stable, as it eliminates the possibility that the referencing compound will interact with the NPs. Such an interaction could significantly reduce the accuracy of an internally referenced system. For these reasons, the Trp referencing system, combined with 2D NMR, provides a superior approach for quantifying peaks compared to the 1D NMR, internally referenced systems used before. The multidimensional approaches enabled by the Trp referencing system also enable measurement on protein mixtures, as described next.

3.2. Competitive Binding of Protein Variants in Mixtures. One of the main benefits of multidimensional NMR spectroscopy is the ability to resolve signals corresponding to individual protein residues. When multiple proteins are present, non-overlapping signals can be used to monitor the behavior of two, three, or even more proteins simultaneously in the same sample. Until now, quantitation of multiple proteins in the presence of NPs has been limited to 1D NMR, where each protein is isotopically labeled with either ^{13}C or ^{15}N.[32] Practically, this approach limits measurements of protein−NP binding to mixtures of only two proteins using NMR, and the expense of expressing ^{13}C-labeled protein is significantly higher than labeling with ^{15}N. Monitoring how complex mixtures of

https://doi.org/10.1021/acs.analchem.1c01911
Anal. Chem. 2021, 93, 11982−11990

proteins interact with NPs is important, and it is increasingly recognized that multiple protein competition is critical in the formation of the in vivo NP corona.[12,16]

To this end, the Trp referencing system was tested with two competitive protein binding experiments. First, Figure 2A shows a quantitative binding experiment where an equal amount of deuterated, ^{15}N-labeled GB3 (^{15}N, ^{2}H, or GB3-D) was in competition with non-deuterated, ^{15}N-labeled GB3 (^{15}N, ^{1}H, or GB3-H). In this experiment, perdeuteration of GB3-D introduces a small upfield shift in the ^{15}N chemical shifts,[37] and TROSY-HSQC NMR spectroscopy is used to differentiate these chemical shift differences. As shown in Figure 2A, the deuterium shifts for GB3-D and GB3-H are extremely small, but they are resolvable using the TROSY-HSQC and Trp reference. This approach therefore enables quantifying a protein in competition with itself, the only difference being slightly shorter C−D bond length relative to C−H.[37] After the addition of AuNPs, the peak intensities of each residue from both GB3-D and GB3-H are reduced, and normalization of peak intensities relative to the external Trp reference enables a comparison of binding. Again, a decrease in the signal intensity quantitatively corresponds to the AuNP-bound protein for this system. Here, the signal intensities with and without AuNPs (I/I_0) reveal that GB3-H and GB3-D appear to bind in a similar fashion when competing for the same AuNP surface. The average I/I_0 of GB3-H and GB3-D for all residues are 0.85 ± 0.04 and 0.84 ± 0.04, respectively, and the small standard deviations indicate that all residues are affected in the same way (Figure 2B). This result indicates that GB3-H and GB3-D bind AuNPs with roughly the same affinity, which is expected since they are structurally identical.

In a second series of experiments, we examined how ^{15}N-labeled GB3 competes with ^{15}N-labeled Ubq for a limited amount of AuNP surface (Figure 2C). Here, GB3 and Ubq compete very differently. Their binding amounts were compared using a static, low-resolution SOFAST-HMQC measurement (total NMR acquisition time ~6 min) in the presence of 80 nM AuNPs. Under these conditions, 29/72 peaks from Ubq and 25/56 peaks from GB3 can be sufficiently resolved for quantitative analysis (Figure 2D). As shown in the overlay spectra of mixture proteins before binding (red) and after binding (blue) in Figure 2C, no significant chemical shifts are observed in the positions of the protein peaks, consistent with previous 1D measurements of GB3 and Ubq in the presence of AuNPs, both alone and in competition.[31,32] Subsequently, the peak intensities of proteins in the control and competitive binding samples were normalized by the Trp reference signal and converted to relative intensities to quantify the binding amount. Consistent with measurements collected using 1D NMR,[32] the relative intensities of all Ubq peaks (0.74 ± 0.07) are higher than those of GB3 (0.51 ± 0.03), indicating that GB3 has a stronger affinity for AuNPs than Ubq under these conditions. Once again, the peak intensities are largely uniform for both proteins (Figure 2D); however, a small region in the loop between strands β4 and β5 (residues 60−64) shows slightly lower intensity than the other residues. Two of these peaks (Q62, E64) are marginally overlapped with GB3 signals (Figure 2C), which may artificially reduce their intensities. Thus, combined with the comparison of GB3-H and GB3-D, these results demonstrate the utility of the external Trp reference in reliably quantifying signals for each residue in a mixture of proteins and NPs in situ.

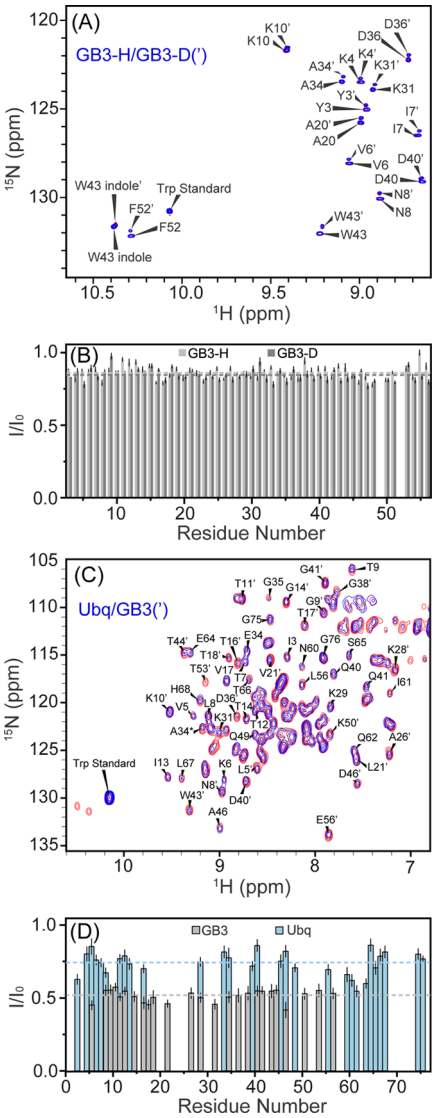

Figure 2. Competitive protein−NP interactions determined using 2D NMR spectroscopy with the Trp reference. (A) Competitive binding study of 20 μM non-deuterated GB3 (GB3-H) and 20 μM deuterated (GB3-D) mixing with 40 nM 15 nm AuNP. This panel shows part of the overlay of the TROSY-HSQC spectra of GB3-D and GB3-H mixtures with (blue) and without (red) AuNPs. The residues highlighted with (') belong to GB3-D. The full spectra are presented in Figure S6, Supporting Information. (B) Relative peak intensities of each residue in GB3-H (light gray) and GB3-D (black) after binding with AuNPs. (C) Competitive binding study of 20 μM GB3 and 20 μM Ubq onto 80 nM 15 nm AuNPs at pH 6.5 using SOFAST-HMQC. The overlay spectra of protein mixtures with and without AuNPs are color coded in blue and red, respectively. The assignments are indicated for only the well-resolved peaks in the mixture of Ubq and GB3 (primed residues) after mixing with AuNPs. (D) Relative peak intensities of the well-resolved residues shown in (C) after binding with AuNPs. The dashed lines indicate the average relative intensity for Ubq (blue) and GB3 (light gray). All experiments are conducted thrice, and the error bars represent the standard deviation of three replicates.

3.3. Kinetic Measurements of Protein Competitive Adsorption. Finally, we examined the utility of the Trp reference for time-resolved studies of protein−NP binding. This simple system, where two different proteins compete for the surface of an AuNP, could potentially be extended to

https://doi.org/10.1021/acs.analchem.1c01911
Anal. Chem. 2021, 93, 11982−11990

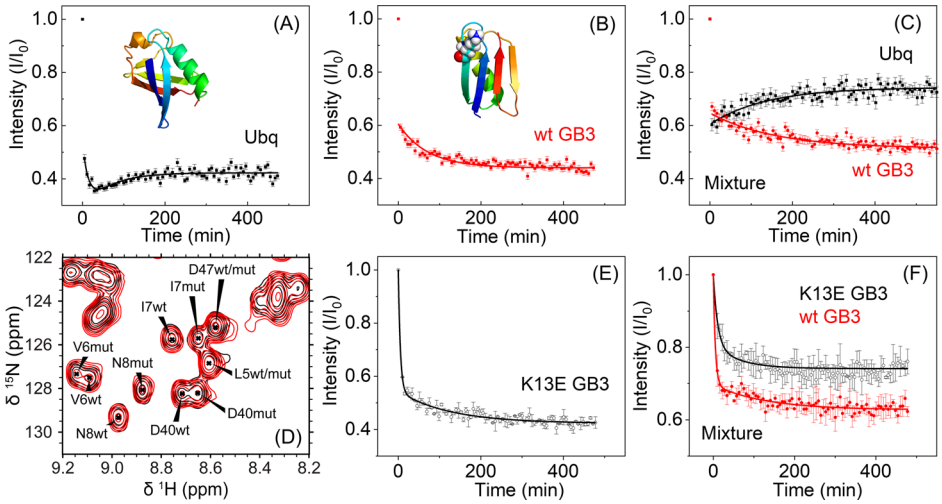

Figure 3. Kinetic studies of competitive binding of multiple proteins onto 15 nm AuNPs at pH 6.5 using SOFAST-HMQC. (A) Peak intensity for 20 μM Ubq as a function of time after mixing with 80 nM AuNPs. The image shows the secondary structure of Ubq. (B) Peak intensity for 20 μM wt GB3 as a function of time after mixing with AuNPs. The inset shows the structure of wt GB3, with the K13 residue highlighted as CPK spheres. (C) Peak intensities vs time for 20 μM Ubq (black) and 20 μM GB3 (red) residues after mixing with 80 nM AuNPs. Each data point is an average of over 29 well-resolved residues for Ubq and 25 for GB3, respectively. (D) SOFAST-HMQC overlay of a mixture of wt GB3 and K13E GB3 without (red) and with (black) the presence of 80 nM AuNPs. The residues belonging to wt GB3 (wt) and K13E GB3 (mut) are indicated. (E) Peak intensity vs time for 20 μM K13E GB3 after mixing with AuNPs. (F) Peak intensities vs time for 20 μM wt GB3 (red) and 20 μM K13E GB3 (black) residues after mixing with 80 nM AuNPs. The error bars represent the standard error of the mean for two replicates.

understand adsorption in more complex physiological environments. We first investigate a system where Ubq and GB3 compete for binding to an AuNP surface. Next, we investigate an even more challenging system involving two GB3 variants that differ by only a single residue, namely, wt GB3 and K13E GB3.

Our group has attempted previously to follow the competitive binding kinetics of Ubq and GB3 in a mixture in the presence of AuNPs.[32] 1D proton NMR and half-filter experiments were employed to separately collect the spectra of ^{13}C-labeled GB3, ^{15}N-labeled Ubq, and the internal standard for concentration determination. This measurement approach introduces large uncertainties in the determination of the exact binding time for each time point, and it also reduces the time efficiency (it takes ~30 min to acquire three spectra for a single time point). The use of an internal standard, and the potential for that reference to interact with the AuNPs themselves, also complicated sample preparation and data acquisition. Here, we attempt to enhance the time resolution of this competitive binding study by using SOFAST-HMQC with the external Trp standard as the reference of peak intensity. As discussed above, these experiments can be acquired quickly, and signals for all proteins and the Trp reference are collected simultaneously in a single experiment.

The kinetic binding experiments were performed by adding AuNPs to an excess amount of a single protein or a mixture of proteins, and the bound amount of each protein was determined by monitoring the protein signals. The peak intensities for each residue are normalized by the Trp standard prior to being normalized by the signals of the first time point (I/I_0 = 1.0), which corresponds to the intensities of the non-AuNP-containing protein sample (I_0). For all proteins observed (Figure 3), a significant amount of binding occurs in the dead time before the start of acquisition. This is indicated by the difference between the first point and the second point in all experiments.

Distinct binding behaviors are observed for Ubq and GB3 with and without competition. Here, we used pseudo-first-order fitting to estimate the time scales of protein binding (eq 2), with a characteristic time $\tau = k_{on}^{-1}$. All fitting parameters are provided in the Supporting Information. For Ubq and GB3 (Figure 3A–C), models were fit from the second point, instead of the first point, due to the presence of protein displacement observed in competition (Figure 3C). The onset of displacement is lost in the experiment dead time, and excluding the dead time period in the fitting allows us to obtain the adsorption and displacement rate during competition. When only one protein is present, Ubq is adsorbed onto AuNPs at a significantly faster rate than GB3, indicated by the greater loss of signal during the experiment dead time, and the faster reduction of peak intensity in the early binding period (Figure 3A,B). Multiexponential behavior (τ_{fast} and τ_{slow}) was observed for Ubq following the initial drop in intensity, and a single exponential (τ_{slow}) was observed for GB3 after mixing with AuNPs. The fast decay of Ubq has a time constant (τ_{fast}) of 12 ± 6 min. Interestingly, this initial process appears to overshoot the final, steady-state binding, and no similar fast process is observed for GB3. After 10 min, the Ubq signal begins to rise, a feature that is also absent in the GB3 intensities. The mechanistic origin of the biphasic behavior in Ubq is not presently clear. On the one hand, slow reorientation over time on the AuNP surface may slowly displace the bound Ubq, resulting in an increase in signal as more proteins are freed. On the other hand, line broadening may be contributing to the signal integration in a way that we are not able to detect but is nevertheless reflected in the signal intensities. Lundqvist et al. observed the complete loss and recovery of NMR signals of human carbonic anhydrase II on the surface of silica NPs,[43] but in that system, the signal loss lasted for 6–7 days. The slow processes for Ubq and GB3 are similar, with τ_{slow} values of 72 ± 30 and 80 ± 9 min, respectively. This slow process may correspond to the slow rearrangement of proteins that can occur after initial adsorption, making room for more protein

https://doi.org/10.1021/acs.analchem.1c01911
Anal. Chem. 2021, 93, 11982–11990

adsorption (in the case of GB3) or displacing loosely bound protein (in the case of Ubq).[31] At the end of 3 hours, both proteins appear to reach a stable bound fraction on the AuNP surface in the absence of competition.

When equal amounts of both Ubq and GB3 are present to compete for AuNP surface, a displacement process is clearly visualized. Interestingly, the biphasic behavior of Ubq disappears, and while the signal still increases over time, the rapid binding phase for both proteins occurs entirely during the experiment dead time. Ubq binds more in the initial ∼20 min, but subsequently, the initially adsorbed Ubq is gradually displaced by GB3. The GB3 adsorption rate (138 ± 17 min) is comparable to the Ubq desorption rate (148 ± 17 min), strongly suggesting that the decrease and increase are linked to the same process. In other words, GB3 appears to displace Ubq over time. This behavior has been observed before, and it is hypothesized that after binding of Ubq, the net charge of the AuNP surface becomes less negative, allowing GB3 to approach the AuNP surface and displace Ubq due to its higher relative binding affinity.[32] The data presented here are consistent with prior observations that employed 1D NMR spectra. However, these data have improved time resolution, and the measurements are far simpler to obtain than 1D measurements of competition kinetics. This is because the 1D competition approach requires separate ^{13}C- and ^{15}N-labeled proteins, as well as multiple NMR spectra at each time point to record the ^{13}C- and ^{15}N-filtered signals. In contrast, the 2D method proposed here relies exclusively on relatively inexpensive ^{15}N-labeled material, and only a single SOFAST-HMQC spectrum is required, which records both proteins and the reference at each time point simultaneously.

Finally, we tested the proposed referencing system to measure the binding kinetics for highly similar variants of the same protein. This is extremely challenging because the NMR spectra of most proteins will be almost identical if the primary structure only differs by one amino acid residue. An earlier study identified the lysine residue at the 13th position of GB3 as the most critical binding site for citrate-coated AuNP interactions, in part because of its favorable charge and proximity to other Lys residues.[32] As a test, we changed this key binding residue to a glutamic acid (K13E), reversing the charge of this site at neutral pH. In the resulting mixture of K13E/wt GB3, the NMR spectra are characterized by a significant overlap, and only a few residues surrounding the mutagenesis site can be resolved (Figure 3D, expanded view shown in Figure S7, Supporting Information). Only those residues close to residue 13 experience sufficient chemical shift perturbations, and only these residues were used for signal quantification. For wt/K13E GB3 binding, all points including the dead time were fit because no displacement is observed in competition. In the absence of wt GB3, the K13E variant binds with a fast time constant τ_{fast} of 4.1 ± 0.6 min and a slow time constant τ_{slow} of 130 ± 20 min (Figure 3E). These time constants are very similar to those of the single wt GB3 binding (τ_{fast} = 5 ± 1 min and τ_{slow} = 130 ± 40 min) (Table S2, Supporting Information). Mutagenesis does not appear to change the binding kinetics in the absence of competition.

As indicated by the Trp-calibrated peak intensities (Figure 3F), when both proteins compete for the same surface, more wt GB3 binds to AuNPs than K13E GB3 after binding has stabilized, reflecting that the Glu residue disrupts charge−charge interactions in binding. A biexponential process fitting (τ_{fast} and τ_{slow}) indicates the τ_{fast} for wt GB3 and K13E GB3 is 5 ± 1 and 10 ± 3 min, respectively. This appears to reflect a kinetically controlled process, where the first protein to reach the AuNP surface is highly favored to adsorb and stay bound during the course of the experiment. In contrast to the GB3/Ubq competition (Figure 3C), no further protein displacement occurs once one GB3 variant is attached to the surface, and the curves in Figure 3F both decrease monotonically over time. The kinetic constants for the second phase of binding for the wt/K13E competition are statistically similar with τ_{slow} values of 130 ± 40 and 160 ± 30 min for wt GB3 and K13E GB3, respectively. Note that the combined bound amount of GB3 variants (∼15% of 20 μM K13E and ∼35% of 20 μM wt GB3 bound, Figure 3F) equals the single-protein GB3 binding capacity (∼55% of 20 μM bound) in Figure 3B,E, as measured by the decrease in signal. This demonstrates consistency in kinetic control since on an average, ∼50% of the available GB3 molecules (wt and variant) are always bound, which also reflects the accuracy of the Trp referencing system. On the other hand, the Ubq/GB3 competitive binding has an element of thermodynamic control since GB3 is able to displace adsorbed Ubq.

The results in this section highlight the importance of studying protein binding in the context of competition by demonstrating that the thermodynamic and kinetic binding behaviors of a single protein in solution do not necessarily represent that protein's actual behavior in a mixture. Studying proteins in complex mixtures can present a significant analytical challenge, and the external Trp referencing system, combined with multidimensional NMR, is able to quantify a variety of new protein competitive binding behaviors, which until now have been challenging to observe spectroscopically.

4. CONCLUSIONS

A ^{15}N tryptophan compound is proposed as an external reference for quantitative NMR studies of protein−NP interactions using two-dimensional ^{1}H−^{15}N experiments. We validate this approach using single-protein titrations in the presence of AuNPs, demonstrating that observed binding capacities are consistent with previously obtained results with better precision. In addition, competitive protein binding experiments also agree with previous results, and the novel Trp referencing system proposed makes such measurements far more accessible. After validation, we demonstrate that the Trp referencing system can be used to study the binding kinetics of two proteins to a single NP. The time resolution of these experiments is vastly improved compared to prior work, and mixtures of three or more proteins are possible depending on the overlap of NMR spectral signals. Importantly, the protein signal reduction due to adsorption within the first hour of binding is accurately quantified, enabling the ability to differentiate thermodynamic versus kinetic aspects of binding, even in proteins with highly similar spectral signals. Drastically different competing processes are observed between two different proteins (Ubq vs GB3) and two protein variants differing by only one residue (wt GB3 vs K13E GB3). In Ubq/GB3 competition, Ubq is first drawn to the AuNP due to the kinetically favorable electrostatic attraction, but it is subsequently displaced by GB3, which has a higher binding affinity. In contrast, the wt/K13E GB3 competition is entirely kinetically controlled. This work demonstrates that the external Trp standard can be readily applicable as an important referencing tool in a wide range of quantitative NMR studies of the NP protein corona.

https://doi.org/10.1021/acs.analchem.1c01911
Anal. Chem. 2021, 93, 11982−11990

■ ASSOCIATED CONTENT

Supporting Information

The Supporting Information is available free of charge at https://pubs.acs.org/doi/10.1021/acs.analchem.1c01911.

Mutagenesis of wt GB3 to obtain K13E GB3; synthesis and characterization of AuNPs; experimental details for NMR experiments; effect of relaxation on data quantification using the Trp standard; practical considerations of NMR data processing with the Trp standard; determination of binding capacities for GB3 and Ubq; TROSY spectra of GB3-D and GB3-H mixtures; and fitting of kinetic data for multiprotein competitive binding (PDF)

■ AUTHOR INFORMATION

Corresponding Author

Nicholas C. Fitzkee − *Department of Chemistry, Mississippi State University, Starkville, Mississippi 39762, United States;* orcid.org/0000-0002-8993-2140; Phone: 662-325-1288; Email: nfitzkee@chemistry.msstate.edu

Authors

Joanna Xiuzhu Xu − *Department of Chemistry, Mississippi State University, Starkville, Mississippi 39762, United States*

Md. Siddik Alom − *Department of Chemistry, Mississippi State University, Starkville, Mississippi 39762, United States*

Complete contact information is available at: https://pubs.acs.org/10.1021/acs.analchem.1c01911

Author Contributions

†J.X.X. and M.S.A. contributed equally to this work. J.X.X., M.S.A., and N.C.F. designed and performed the experiments. J.X.X. and N.C.F. wrote the manuscript.

Notes

The authors declare no competing financial interest.

■ ACKNOWLEDGMENTS

We thank Dr. Jinfa Ying for the helpful discussion and assistance with the sensitivity-enhanced SOFAST-HMQC processing script. This work was supported by the National Institute of Allergy and Infectious Diseases of the National Institutes of Health under grant number R01AI139479 and the National Science Foundation under grant number MCB 1818090. The content is solely the responsibility of the authors and does not necessarily represent the official views of the National Institutes of Health or National Science Foundation.

■ REFERENCES

(1) Liu, N.; Tang, M.; Ding, J. *Chemosphere* **2020**, *245*, 125624.

(2) Anselmo, A. C.; Mitragotri, S. *Bioeng. Transl. Med.* **2019**, *4*, No. e10143.

(3) Pelaz, B.; Alexiou, C.; Alvarez-Puebla, R. A.; Alves, F.; Andrews, A. M.; Ashraf, S.; Balogh, L. P.; Ballerini, L.; Bestetti, A.; Brendel, C.; Bosi, S.; Carril, M.; Chan, W. C. W.; Chen, C.; Chen, X.; Chen, X.; Cheng, Z.; Cui, D.; Du, J.; Dullin, C.; Escudero, A.; Feliu, N.; Gao, M.; George, M.; Gogotsi, Y.; Grünweller, A.; Gu, Z.; Halas, N. J.; Hampp, N.; Hartmann, R. K.; Hersam, M. C.; Hunziker, P.; Jian, J.; Jiang, X.; Jungebluth, P.; Kadhiresan, P.; Kataoka, K.; Khademhosseini, A.; Kopeček, J.; Kotov, N. A.; Krug, H. F.; Lee, D. S.; Lehr, C.-M.; Leong, K. W.; Liang, X.-J.; Ling Lim, M.; Liz-Marzán, L. M.; Ma, X.; Macchiarini, P.; Meng, H.; Möhwald, H.; Mulvaney, P.; Nel, A. E.; Nie, S.; Nordlander, P.; Okano, T.; Oliveira, J.; Park, T. H.; Penner, R. M.; Prato, M.; Puntes, V.; Rotello, V. M.; Samarakoon, A.; Schaak, R. E.; Shen, Y.; Sjöqvist, S.; Skirtach, A. G.; Soliman, M. G.; Stevens, M. M.; Sung, H.-W.; Tang, B. Z.; Tietze, R.; Udugama, B. N.; VanEpps, J. S.; Weil, T.; Weiss, P. S.; Willner, I.; Wu, Y.; Yang, L.; Yue, Z.; Zhang, Q.; Zhang, Q.; Zhang, X.-E.; Zhao, Y.; Zhou, X.; Parak, W. J. *ACS Nano* **2017**, *11*, 2313−2381.

(4) Day, J. P. R.; Rago, G.; Domke, K. F.; Velikov, K. P.; Bonn, M. *J. Am. Chem. Soc.* **2010**, *132*, 8433−8439.

(5) Bajgiran, K. R.; Dorman, J. A.; Melvin, A. T. *ACS Sens.* **2020**, *5*, 29−33.

(6) Schöttler, S.; Becker, G.; Winzen, S.; Steinbach, T.; Mohr, K.; Landfester, K.; Mailänder, V.; Wurm, F. R. *Nat. Nanotechnol.* **2016**, *11*, 372−377.

(7) Corbo, C.; Molinaro, R.; Tabatabaei, M.; Farokhzad, O. C.; Mahmoudi, M. *Biomater. Sci.* **2017**, *5*, 378−387.

(8) Yang, S.-T.; Liu, Y.; Wang, Y.-W.; Cao, A. *Small* **2013**, *9*, 1635−1653.

(9) Chanana, M.; Correa-Duarte, M. A.; Liz-Marzán, L. M. *Small* **2011**, *7*, 2650−2660.

(10) Chen, F.; Wang, G.; Griffin, J. I.; Brenneman, B.; Banda, N. K.; Holers, V. M.; Backos, D. S.; Wu, L.; Moghimi, S. M.; Simberg, D. *Nat. Nanotechnol.* **2017**, *12*, 387−393.

(11) Kurtz-Chalot, A.; Villiers, C.; Pourchez, J.; Boudard, D.; Martini, M.; Marche, P. N.; Cottier, M.; Forest, V. *Mater. Sci. Eng., C* **2017**, *75*, 16−24.

(12) Mahmoudi, M.; Lynch, I.; Ejtehadi, M. R.; Monopoli, M. P.; Bombelli, F. B.; Laurent, S. *Chem. Rev.* **2011**, *111*, 5610−5637.

(13) Simon, J.; Kuhn, G.; Fichter, M.; Gehring, S.; Landfester, K.; Mailänder, V. *Cells* **2021**, *10*, 132.

(14) Moon, D. W.; Park, Y. H.; Lee, S. Y.; Lim, H.; Kwak, S.; Kim, M. S.; Kim, H.; Kim, E.; Jung, Y.; Hoe, H.-S.; Kim, S.; Lim, D.-K.; Kim, C.-H.; In, S.-I. *ACS Appl. Mater. Interfaces* **2020**, *12*, 18056−18064.

(15) Pinals, R. L.; Yang, D.; Rosenberg, D. J.; Chaudhary, T.; Crothers, A. R.; Iavarone, A. T.; Hammel, M.; Landry, M. P. *Angew. Chem., Int. Ed.* **2020**, *59*, 23668−23677.

(16) Monopoli, M. P.; Walczyk, D.; Campbell, A.; Elia, G.; Lynch, I.; Baldelli Bombelli, F.; Dawson, K. A. *J. Am. Chem. Soc.* **2011**, *133*, 2525−2534.

(17) Pustulka, S. M.; Ling, K.; Pish, S. L.; Champion, J. A. *ACS Appl. Mater. Interfaces* **2020**, *12*, 48284−48295.

(18) Petkova, G. A.; Záruba, K.; Žvátora, P.; Král, V. *Nanoscale Res. Lett.* **2012**, *7*, 287.

(19) Yang, J. A.; Johnson, B. J.; Wu, S.; Woods, W. S.; George, J. M.; Murphy, C. J. *Langmuir* **2013**, *29*, 4603−4615.

(20) Johnson, W. C., Jr. *Annu. Rev. Biophys. Biophys. Chem.* **1988**, *17*, 145−166.

(21) Sheibani, S.; Basu, K.; Farnudi, A.; Ashkarran, A.; Ichikawa, M.; Presley, J. F.; Bui, K. H.; Ejtehadi, M. R.; Vali, H.; Mahmoudi, M. *Nat. Commun.* **2021**, *12*, 573.

(22) Zhang, C.; Li, X.; Wang, Z.; Huang, X.; Ge, Z.; Hu, B. *J. Phys. Chem. B* **2020**, *124*, 684−694.

(23) Lacerda, S. H. D. P.; Park, J. J.; Meuse, C.; Pristinski, D.; Becker, M. L.; Karim, A.; Douglas, J. F. *ACS Nano* **2010**, *4*, 365−379.

(24) Zhang, X.; Shi, H.; Zhang, R.; Zhang, J.; Xu, F.; Qiao, L.; Yu, S. *Part. Part. Syst. Charact.* **2019**, *36*, 1800257.

(25) Assfalg, M.; Ragona, L.; Pagano, K.; D'Onofrio, M.; Zanzoni, S.; Tomaselli, S.; Molinari, H. *Biochim. Biophys. Acta, Proteins Proteomics* **2016**, *1864*, 102−114.

(26) Anthis, N. J.; Clore, G. M. *Q. Rev. Biophys.* **2015**, *48*, 35−116.

(27) Ceccon, A.; Tugarinov, V.; Bax, A.; Clore, G. M. *J. Am. Chem. Soc.* **2016**, *138*, 5789−5792.

(28) Xie, M.; Yu, L.; Bruschweiler-Li, L.; Xiang, X.; Hansen, A. L.; Brüschweiler, R. *Sci. Adv.* **2019**, *5*, No. eaax5560.

(29) Wardenfelt, S.; Xiang, X.; Xie, M.; Yu, L.; Bruschweiler-Li, L.; Brüschweiler, R. *Angew. Chem., Int. Ed.* **2021**, *60*, 148−152.

(30) Perera, Y. R.; Hill, R. A.; Fitzkee, N. C. *Isr. J. Chem.* **2019**, *59*, 962−979.

(31) Wang, A.; Vangala, K.; Vo, T.; Zhang, D.; Fitzkee, N. C. *J. Phys. Chem. C* **2014**, *118*, 8134−8142.
(32) Wang, A.; Perera, Y. R.; Davidson, M. B.; Fitzkee, N. C. *J. Phys. Chem. C* **2016**, *120*, 24231−24239.
(33) Woods, K. E.; Perera, Y. R.; Davidson, M. B.; Wilks, C. A.; Yadav, D. K.; Fitzkee, N. C. *J. Phys. Chem. C* **2016**, *120*, 27944−27953.
(34) Frens, G. *Nat. Phys. Sci.* **1973**, *241*, 20−22.
(35) Turkevich, J.; Stevenson, P. C.; Hillier, J. *Discuss. Faraday Soc.* **1951**, *11*, 55−75.
(36) Pervushin, K.; Riek, R.; Wider, G.; Wüthrich, K. *Proc. Natl. Acad. Sci. U.S.A.* **1997**, *94*, 12366−12371.
(37) Jameson, C. J. Isotope Effects on Chemical Shifts and Coupling Constants. *Encyclopedia of Nuclear Magnetic Resonance*, 4th ed.; Wiley: New York, 1996; Vol. *4*, pp 2638−2655.
(38) Schanda, P.; Brutscher, B. *J. Am. Chem. Soc.* **2005**, *127*, 8014−8015.
(39) Kern, T.; Schanda, P.; Brutscher, B. *J. Magn. Reson.* **2008**, *190*, 333−338.
(40) Palmer, A. G.; Cavanagh, J.; Wright, P. E.; Rance, M. *J. Magn. Reson.* **1991**, *93*, 151−170.
(41) Schanda, P.; Kupče, Ē.; Brutscher, B. *J. Biomol. NMR* **2005**, *33*, 199−211.
(42) O'Neil, M. J. *The Merck Index: An Encyclopedia of Chemicals, Drugs, and Biologicals*; Royal Society of Chemistry: Cambridge, UK, 2006.
(43) Lundqvist, M.; Sethson, I.; Jonsson, B.-H. *Langmuir* **2005**, *21*, 5974−5979.

https://doi.org/10.1021/acs.analchem.1c01911
Anal. Chem. 2021, 93, 11982−11990